

RESEARCH

Open Access



Targeting EP300 in diffuse large b-cell lymphoma: efficacy of A485 and synergistic effects with XPO1 inhibition

Yanan Jiang^{1†}, Donghui Xing^{2†}, Xiang He², Wenqi Wu³, Hong Xu², Huimeng Sun², Yixin Zhai², Kaiping Luo² and Zhigang Zhao^{1,2*}

Abstract

Background Diffuse large B-cell lymphoma (DLBCL) is an aggressive hematopoietic malignancy, necessitating the exploration of innovative therapeutic approaches. Targeting epigenetic mechanisms has emerged as a promising avenue for cancer treatment. EP300 belongs to the KAT3 family of histone/non-histone lysine acetyltransferases, regulating gene expression by acetylating H3K27. However, the role of EP300 and its potential as a targeted therapy in DLBCL remains unknown.

Methods Public datasets were collected to evaluate the expression and clinical significance of epigenetic modification-related genes in patients with DLBCL. Flow cytometry, colony formation, and western blotting were conducted to investigate the function of EP300. CCK8, proliferation, cell cycle, and apoptosis assays, as well as experiments in tumor-bearing mouse models were conducted to determine the therapeutic effect of the EP300 inhibitor A485 alone or in combination with the XPO1 inhibitor KPT8602. RNA-seq was used to investigate the molecular mechanisms underlying the inhibition of DLBCL development by A485.

Results EP300 is frequently overexpressed in DLBCL and is associated with poor prognosis, highlighting its potential role in lymphoma progression. In this study, we found that A485, a novel small-molecule inhibitor targeting the conserved histone acetyltransferase (HAT) domain of EP300, significantly reduced H3K27Ac levels and demonstrated potent antitumor effects in DLBCL cells, both in vitro and in vivo. Furthermore, we showed that A485 attenuated DLBCL progression by inhibiting the MYC and E2F1 pathways. Notably, the combination of A485 with the XPO1 inhibitor KPT8602 produced synergistic anti-lymphoma in vitro and in vivo effects in DLBCL cell lines. This combination therapy resulted in enhanced tumor suppression in a DLBCL xenograft model with minimal toxicity. These findings suggested that targeting EP300, particularly in conjunction with XPO1 inhibition, could represent a promising therapeutic strategy for DLBCL treatment.

Conclusions Our study elucidated that EP300 inhibition, especially in combination with XPO1 blockade, could serve as a promising therapeutic strategy for the treatment of DLBCL.

[†]Yanan Jiang and Donghui Xing contributed equally to this work.

*Correspondence:
Zhigang Zhao
zzhao01@tmu.edu.cn

Full list of author information is available at the end of the article



© The Author(s) 2025. **Open Access** This article is licensed under a Creative Commons Attribution-NonCommercial-NoDerivatives 4.0 International License, which permits any non-commercial use, sharing, distribution and reproduction in any medium or format, as long as you give appropriate credit to the original author(s) and the source, provide a link to the Creative Commons licence, and indicate if you modified the licensed material. You do not have permission under this licence to share adapted material derived from this article or parts of it. The images or other third party material in this article are included in the article's Creative Commons licence, unless indicated otherwise in a credit line to the material. If material is not included in the article's Creative Commons licence and your intended use is not permitted by statutory regulation or exceeds the permitted use, you will need to obtain permission directly from the copyright holder. To view a copy of this licence, visit <http://creativecommons.org/licenses/by-nc-nd/4.0/>.

Keywords DLBCL, EP300, Epigenetics, A485, Histone acetyltransferases

Background

Diffuse large B-cell lymphoma (DLBCL) is the most prevalent subtype of aggressive lymphoma, accounting for approximately 30% of newly diagnosed cases annually [1]. While most patients with DLBCL are successfully treated with anthracycline-based combination chemotherapy and the monoclonal antibody rituximab, approximately 40% relapse following standard first-line therapy [2]. Despite significant advancements in therapeutic approaches, including chemoimmunotherapy and targeted agents, challenges remain in achieving durable remission and improving the overall survival rates in these patients [3–5].

Recent studies have highlighted the crucial role of epigenetic alterations, such as aberrant DNA methylation and histone modifications, in the pathogenesis of DLBCL [6, 7]. A deeper understanding of these epigenetic changes and their underlying mechanisms may facilitate the development of novel therapeutic strategies. Histone acetylation, the most prevalent epigenetic change, is dynamically regulated by histone deacetylases (HDACs). This modification governs access to chromatin, facilitating gene transcription, DNA replication, and repair [8]. Abnormal histone acetylation is a critical early event in tumorigenesis. Previous studies have demonstrated that H3K27ac is associated with the occurrence and progression of various human tumors, including breast cancer and hepatocellular carcinoma (HCC) [9, 10]. Totani et al. found that H3K27ac/BRD4 epigenetics regulate the HGF/c-MET pathway in adult T-cell lymphoma/leukemia [11]. Sungalee et al. confirmed that the dynamics of H3K27ac enrichment mediate the interaction frequency between regulatory regions, leading to allele-specific chromatin configurations that promote oncogene expression in B-cell lymphomas [12]. Epigenetic agents leverage the plasticity of the epigenome to reprogram cellular phenotypes, exhibiting significant anti-tumor activity. Growing evidence has shown that HDAC inhibitors (HDACis), either alone or in combination, have emerged as promising therapeutic options for hematological malignancies [13–16]. Recently, there has been an increasing focus on understanding the role of histone acetylation modifications and their targeted therapies in cancer.

EP300 and its closely related homolog cAMP response element-binding protein-binding protein (CREBBP) belong to the KAT3 family of histone and non-histone lysine acetyltransferases, regulating gene expression through the acetylation of H3K27 and acting as transcriptional coactivators by interacting with various transcription factors (TFs) [17]. Numerous studies have established that EP300 is closely associated with tumor

growth, proliferation, and survival. For instance, Cai et al. found that p300/CBP-mediated acetylation of H3K18 and H3K27 is increased in HCC and that targeting p300/CBP attenuates HCC progression through the epigenetic regulation of metabolism [10]. Welti et al. reported that the inhibition of EP300/CREBBP leads to reduced H3K27ac levels, subsequently inhibiting growth and androgen receptor (AR) activity in castration-resistant prostate cancer [18]. Additionally, studies have shown that EP300 is essential for maintaining the oncogenic potential of leukemia stem cells (LSCs), and the EP300 inhibitor A485 potentially affects LSC growth by targeting enhancer activity through histone acetyltransferase (HAT) domain inhibition [19]. However, the role of EP300 and its potential therapeutic targets in DLBCL remains unexplored.

In this study, we investigated the therapeutic potential of A485, a novel small-molecule inhibitor of the EP300 conserved HAT domain, either alone or in combination with other small-molecule inhibitors. These findings may provide insights for future drug development and treatment strategies.

Methods

Cell lines

TMD8, OCI-LY7, U2932, OCI-LY3, and Pfeiffer cells were generously provided by the Basic Laboratory of Tianjin Medical University. TMD8, Pfeiffer, OCI-LY3, and U2932 were maintained in RPMI-1640 medium (Gibco), OCI-LY7 was maintained in IMDM medium (Gibco), supplemented with 10% fetal bovine serum (NEWZERUM), and 1% pen/strep (Gibco) at 37°C and 5% CO₂. The 293T cell was cultured in DMEM (Gibco) supplemented with 10% fetal bovine serum and 1% pen/strep at 37°C and 5% CO₂. These cell lines were negative for mycoplasma through recently testing by the PCR Mycoplasma Test Kit (HUABIO, K0103).

Data analysis

The gene-expression and clinical information of GSE10846 cohort patients were download from <https://portal.gdc.cancer.gov>. High-throughput sequencing data of 47 DLBCL tissues from the TCGA database and 337 normal control tissues were analyzed by GEPIA database (<http://gepia.cancer-pku.cn/>), which developed by a team from Peking University, is an online platform for rapid customized analysis of data from TCGA and GTEx databases. DepMap (<https://depmap.org/portal/>) is a database containing 796 CRISPR screens and 710 RNAi screens datasets. We queried the necessity of genes in various cells using the DepMap database, specifically examining perturbation effects scores, namely

copy number-adjusted dependency scores (CERES), to pre-evaluate the impact of these genes on cellular proliferation phenotypes. CERES score is a computational method to estimate gene dependency levels from CRISPR-Cas9 essentiality screens while accounting for the copy-number-specific effect. A more negative CERES score indicates that the gene is essential for cell viability in the certain cell line. A CERES score of -1 indicates the median of all pan-essential genes. We calculated the CERES score through 898 tumor cell lines including 30 lymphoma cell lines.

Western blotting

DLBCL cell lines were treated with DMSO (control), 250 nM A485, or 500 nM A485 for 72 h. After treatment, cells were harvested, and protein was extracted using RIPA buffer (Solarbio, R0010) supplemented with PMSF (Beyotime, ST506) and a protease inhibitor cocktail (Roche). Protein concentrations were measured, and 20 µg of protein was separated by SDS-PAGE (6–12% gradient gels, Shanghai Epizyme Biomedical Technology). The proteins were then transferred onto Immobilon-P PVDF membranes (Millipore, IPVH00010; 0.45 µm pore size). Membranes were blocked with 5% non-fat milk in TBS-T, incubated with primary antibodies (listed in Supplementary Table S5), and detected using chemiluminescence on the Chemidoc Touch imaging system (Bio-Rad).

Cell viability assay

DLBCL cells were cultured in 96-well plates and treated with serial dilutions of inhibitors. Cell viability was evaluated after 72 h using the CCK8 assay, and optical density was measured according to standard protocols. Inhibitors were sourced from MedChemExpress. Cell growth,

Cell proliferation, cell cycle, and apoptosis analysis

Cell proliferation was evaluated using the EdU assay. Briefly, DLBCL cells were incubated with 10 µM EdU (Beyotime, C0075S) for 2 h, followed by fixation and staining according to the manufacturer's instructions. The proportion of proliferating cells was quantified by flow cytometry (BD FACSCanto II). For cell cycle analysis, cells were fixed in 70% ethanol at 4 °C overnight, treated with RNase A (Solarbio), and stained with propidium iodide (PI) solution (Beyotime, C1052). DNA content was analyzed by flow cytometry, and cell cycle distribution was determined using FlowJo v10. Apoptosis was assessed using the Annexin V-PE/7-AAD Apoptosis Detection Kit (BD Biosciences, 559763) according to the manufacturer's protocol. After staining, apoptotic cells (early and late) were quantified using flow cytometry. Data were analyzed with FlowJo v10.

In vivo treatment

The animal studies and experimental protocols were approved by the Animal Ethical and Welfare Committee of Tianjin Medical University Cancer Institute and Hospital. Female athymic NSG (NOD-Prkdcscid-Il2rgeml) mice (6–8 weeks old) were obtained from SPF (Beijing Biotechnology) and housed in a specific pathogen-free (SPF) environment at the Tianjin Medical University Cancer Institute and Hospital Animal Center, with 5 mice per cage. For tumor xenograft establishment, 1.0×10^7 OCI-LY7 cells were subcutaneously injected into the right flank of the mice. Tumor growth was monitored by measuring the tumor size using Vernier calipers in two dimensions, and tumor volume was calculated using the formula: $\text{volume} = \text{length} \times (\text{width})^2 \times \pi/6$. Once the tumors reached an average volume of approximately 60 mm³, the mice were randomly assigned into two groups (6 animals per group) and treated with DMSO, A485, KPT8602, or a combination of A485 and KPT8602. A485 was administered intraperitoneally at a daily dose of 100 mg/kg, dissolved in a vehicle consisting of 5% DMSO (Solarbio), 40% PEG300 (Sigma), 5% tween-80 (Solarbio), and 50% normal saline. For combination therapy, both the A485 group and the A485 + KPT8602 group received A485 at a reduced dose of 50 mg/kg, using the same solvent mix. KPT8602 was administered orally at a daily dose of 15 mg/kg, using the same solvent mix. After two weeks of treatment, the mice were euthanized. Prior to euthanasia, the mice were deeply anesthetized using isoflurane inhalation to ensure complete unconsciousness and insensitivity to pain. After two weeks of treatment, the mice were sacrificed. Prior to euthanasia, all animals were deeply anesthetized using isoflurane inhalation to ensure they were unconscious and insensible to pain. Euthanasia was performed by cervical dislocation following anesthesia, in accordance with the guidelines approved by the Animal Ethical and Welfare Committee. The tumors were then excised and weighed.

Statistical analysis

Data analyses were performed with Prism 10 (GraphPad software, La Jolla, CA). FDR was adjusted using the Benjamini-Hochberg method for RNA-seq data. Unpaired two-tailed Student's T test was used to analyze the percentage of proliferation, apoptosis, colony number, and expression of mRNA. All measurements are shown as the mean ± SD or mean ± SEM where appropriate. The comparison of expression levels of epigenetic-related genes between DLBCL and normal tissues was conducted using the t-test. Kaplan-Meier method was utilized to plot survival curves, and Log-rank test was employed to analyze the relationship between different factors and overall survival (OS). Statistical significance was set at * $p \leq 0.05$, **

$p \leq 0.01$, and *** $p \leq 0.001$. $p \leq 0.05$ was considered statistically significant.

Results

EP300 correlates with an unfavorable prognosis in DLBCL

Recent studies have highlighted the role of abnormal epigenetic regulation in hematological malignancies. To identify potential epigenetic targets in DLBCL, we analyzed genes involved in epigenetic modifications that were mutated or aberrantly expressed in patients with DLBCL. From 155 frequently altered genes in DLBCL, we identified 15 epigenetic regulator-modifying genes (Fig. 1A; Table 1, Supplementary Table S1-2) [20, 21]. These included *DNMT3A*, *KMT2D*, *EZH2*, *CREBBP*, and *TET2*, which have been associated with prognostic value in hematological malignancies [22, 23]. We subsequently investigated the expression of these genes through the analysis of the mRNA sequencing data from 47 primary DLBCL samples and 337 normal B-cell samples. The results showed that most genes were highly expressed in patients with DLBCL, except *CREBBP*, *KMT2D*, and *TET2*, which were expressed at lower levels in patients with DLBCL, compared to the normal tissues (Fig. 1B). This finding led us to investigate whether there was any correlation between the expression of these genes and the outcomes of patients with DLBCL. By performing survival analysis in 412 well-characterized DLBCL cohorts (GSE10846), we found that patients with higher expression of EP300, DOT1L, DNMT3A, and HDAC3 exhibited significantly inferior overall survival (OS) compared to those with lower expression ($p < 0.05$), indicating enhanced activity of these genes in patients with DLBCL (Fig. 1C). To confirm these findings, we examined the copy number-adjusted dependency scores (CERES) of these 15 genes in lymphoma cell lines using the DepMap exome-wide CRISPR-Cas9 deletion dataset. We observed that the gene dependency scores of HDAC3 and EP300 were the lowest (much lower than 0, even lower than -1), indicating that HDAC3 and EP300 are essential for cell viability in the DLBCL cell line (Fig. 1D). Interestingly, EP300 functions as an “epigenetic writer”, while HDAC3 functions as an “epigenetic eraser”, dynamically controlling histone acetylation modifications and correlating with gene regulation. Aberrant HDAC3 regulation has been linked to lymphoma progression and inhibitors of HDAC3 have been reported as attractive therapies for DLBCL. Compared with the extensively studied HDACs, very little is known about lysine acetyltransferases (KATs) in DLBCL. These findings prompted us to speculate that EP300 could be a therapeutic target.

To address whether the expression of EP300 is a unique feature of DLBCL, we examined its role in different DLBCL subtypes and International Prognostic Index (IPI) groups. EP300^{high} significantly shortened

OS in the ABC-DLBCL, MYC^{high}, and IPI^{high} groups ($p < 0.05$) (Supplementary Fig. S1A). Moreover, we found that, compared to solid tumors, hematopoietic and lymphoid lineages appeared to be more dependent on EP300 (Supplementary Fig. S1B). The combined clinical data suggested that EP300 may play a vital role in DLBCL development. Overall, these observations revealed that EP300 is preferentially overexpressed in patients with DLBCL, and that high expression of EP300 is closely associated with poor prognosis in these patients.

A485 induces pan-subtype growth arrest for DLBCL in vitro and in vivo

The observation that high EP300 expression is closely associated with poor prognosis in patients with DLBCL prompted us to explore this dependency for therapeutic purposes. Although no EP300-specific inhibitors are available, A485 is a clinical candidate HAT domain inhibitor selective for EP300 and CREBBP. We assessed the ability of A485 to inhibit the proliferation of five lymphoma cell lines: OCI-LY7, OCI-LY3, Pfeiffer, U2932, and TMD8. As shown in Fig. 2A, A485 exhibited potent activity against these lymphoma cell lines. We performed flow cytometric analysis to confirm the effect of A485 on lymphoma cells. A485 inhibited DLBCL cell proliferation in a dose-dependent manner (Fig. 2B). The dominant cellular phenotypes of DLBCL cells treated with A485 included prominent G0/G1 cell cycle arrest and the induction of apoptosis (Fig. 2C-D). EP300 inhibition efficiently reduced H3K27Ac deposition in a dose-dependent manner (Fig. 2E). This suggested that the anti-lymphoma activity of A485 may be linked to epigenetic changes involving tumor genes. These data suggested that A485 markedly inhibited the malignant phenotype of DLBCL cells in vitro. To ascertain the antilymphoma activity of A485 in vivo, we developed a xenograft model of a human DLBCL cell line. Tumor-bearing mice were randomized to receive intraperitoneal injections of vehicle or A485. As predicted, significant decreases in tumor progression and weight were observed in the A485 group (Fig. 2F-H). We found no significant alterations in the body weight of the mice, indicating few adverse effects of A485 (Fig. 2I). These data suggested that A485 exerts a selective anti-lymphoma effect on human DLBCL cells both in vitro and in vivo.

Targeting EP300 attenuates lymphoma cell proliferation through inhibition of C-MYC and E2F1 signaling pathways

To further elucidate the mechanism underlying the function of A485, the DLBCL cell line OCI-LY7 was selected to investigate the impact of A485 treatment on its transcriptional networks through RNA sequencing (at the derived IC₅₀ of 500 nmol/L for 72 h). RNA seq experiments were performed in duplicates. We chose

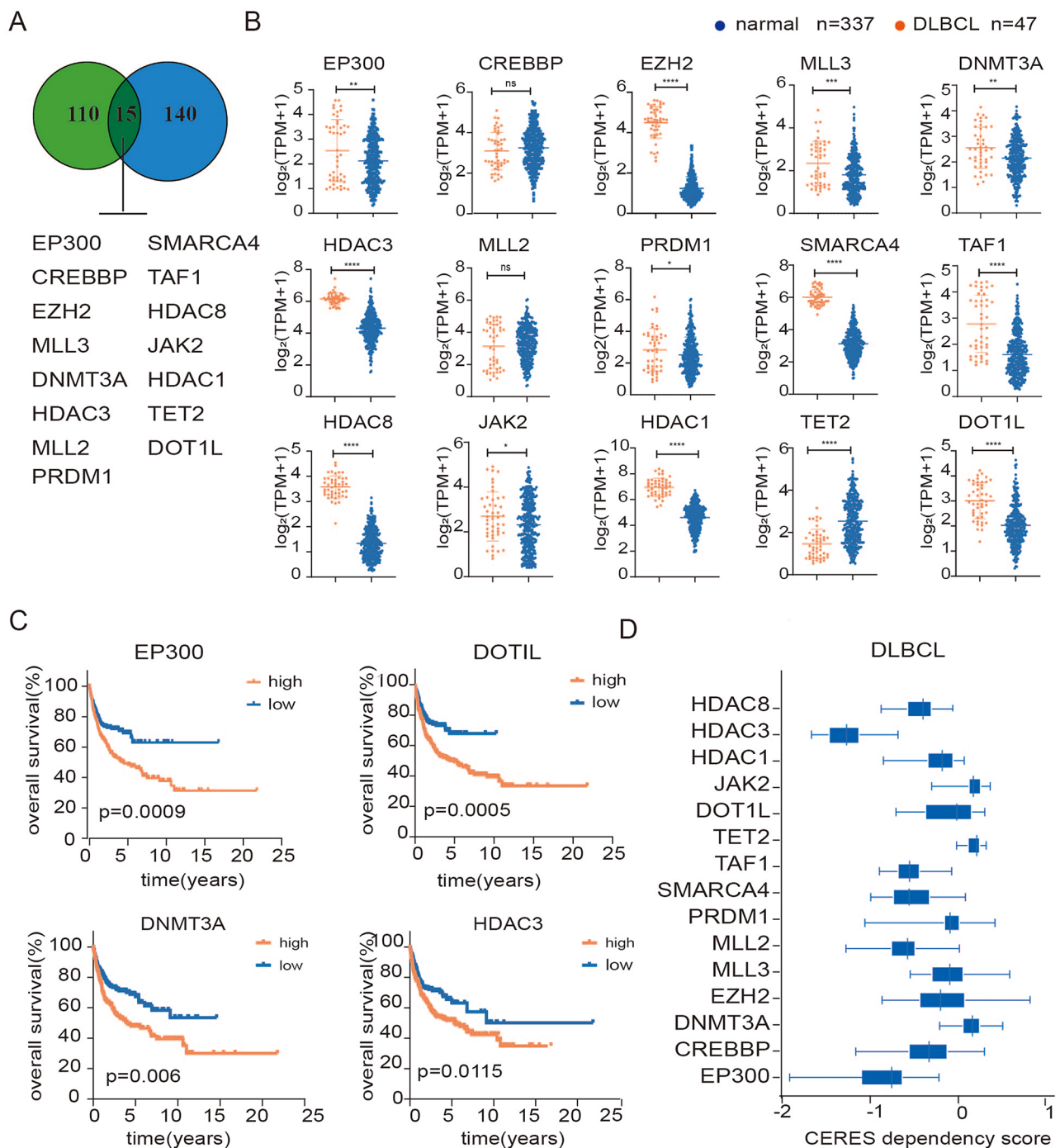


Fig. 1 EP300, a critical epigenetic regulator, correlates with unfavorable prognosis in DLBCL. **A** Venn diagram illustrates epigenetic genes with mutations or aberrant expression in patients with DLBCL. **B** Scatter plots displaying the relative expression levels of 15 epigenetic genes, including EP300, in DLBCL and normal tissues. **C** The impact of epigenetic gene expression on patient survival, with OS curves for DOT1L, EP300, DNMT3A, and HDAC3. According to the median value of gene expression, we divided the study population into high- and low-expression groups, which are represented by red and blue curves, respectively. **D** Copy number-adjusted dependency scores (CERES) of EP300 and other lymphoma-related genes. CERES; a normalized metric of gene essentiality

this cell line because it presented a strong sensitivity to A485, at the same time allowing us to collect sufficient live cells for downstream studies. Significant transcriptional alterations were identified following inhibition

of EP300 activity in these cells, with 1,101 transcripts induced and 1,105 repressed (Fig. 3A, Supplementary Table S3, fold change (FC) ≥ 1 and false discovery rate (FDR) ≤ 0.05). Since EP300, as a histone acetyltransferase,

Table 1 15 epigenetic regulated genes, which May play a role in the prognosis of DLBCL

GENE NAME	DESCRIPTION	SUBTYPE
DNMT3A	DNA Methyltransferase	mutation
CREBBP	Histone Lysine Acetyltransferase	mutation
EP300	Histone Lysine Acetyltransferase	mutation
TAF1	TATA-Box Binding Protein Associated Factor	mutation
HDAC1	Histone Deacetylase	abnormal expression
HDAC3	Histone Deacetylase	abnormal expression
HDAC8	Histone Deacetylase	abnormal expression
MLL2	Histone Methyltransferase	mutation
MLL3	Histone Methyltransferase	mutation
EZH2	Histone Methyltransferase	mutation
PRDM1	Histone Methyltransferase	mutation
SMARCA4	Bromodomain and Extra-Terminal motif proteins	mutation
TET2	TET Methylcytosine Dioxygenase	mutation
JAK2	Tyrosine-Protein Kinase	mutation
DOT1L	Histone Methyltransferase	abnormal expression

is mostly involved in gene activation, we focused on genes downregulated by A485. Gene Ontology (GO) analysis revealed that the differentially downregulated genes with $p\text{-value} < 0.05$ were enriched in biological processes, including cell division, DNA repair, and the cell cycle (Fig. 3B). Kyoto Encyclopedia of Genes and Genomes (KEGG) enrichment analyses performed using the DAVID database also showed that the downregulated genes were mainly enriched in DNA replication, cell cycle, and base excision repair (Fig. 3B).

To investigate pathways associated with the gene expression changes observed, gene set enrichment analysis (GSEA) was performed using the Hallmarks gene set from the Molecular Signatures Database. Few pathways were enriched after A485 treatment. Critically, genes with attenuated enrichment after A485 treatment included the MYC target pathways, oxidative phosphorylation, and E2F target gene sets (Fig. 3C-D, Supplementary Table S4). Numerous studies have indicated that MYC and E2F1 are critical for the survival of patients with DLBCL, and some studies have shown that A485 potentially inhibits MYC expression through decreasing histone acetylation. The ability of A485 to inhibit MYC protein expression in DLBCL cells was confirmed using immunoblotting. We found that the protein expression of MYC was decreased in DLBCL cells treated with A485 compared to that in the controls (Fig. 4A). Strikingly, we found that the protein expression of E2F1 also decreased (Fig. 4B). Increasing evidence suggests that E2F1 is closely associated with tumorigenesis in various cancer

types. Next, we investigated the expression profile of E2F1 and the survival outcomes in patients with DLBCL. Our analysis revealed significant over-expression of E2F1 in DLBCL tissues, and DLBCL patients overexpressing E2F1 had a worse OS ($HR=1.84, 95\%:1.34-2.52, P<0.001$) (Fig. 4C-D). These data indicated that MYC and E2F1 are direct transcriptional targets of A485, which is required for the proliferation and survival of DLBCL cells.

Notably, GO and KEGG analyses revealed that A485 inhibited metabolic pathways, including cholesterol biosynthesis, steroid biosynthesis, carbon metabolism, glycolysis, amino acid biosynthesis, and pyruvate metabolism. GSEA also showed that A485 regulated essential enzyme gene expression in the metabolic processes of DLBCL cells, including oxidative phosphorylation, adipogenesis, and glycolysis. To determine the influence of A485 on the metabolism of DLBCL cells, we conducted GSEA on metabolic gene sets. Consistently, the analysis showed that A485 regulated genes primarily involved in the Tricarboxylic Acid Cycle (TCA), nucleotide metabolism, carbohydrate metabolism, and metabolism of vitamins and cofactors (Supplementary Fig. S3A). We speculated that A485 reduced the expression of metabolic genes by inhibiting EP300/CREBBP-induced histone acetylation. However, further studies are needed to verify this hypothesis.

Simultaneous targeting of EP300 and XPO1 is an effective treatment strategy for DLBCL

A485 inhibited the proliferation of DLBCL cells by targeting EP300, with its effects partly attributed to the suppression of MYC expression. Meanwhile, exportin-1 (XPO1) is a key mediator of nuclear export of various proteins and RNA. It plays a critical role in maintaining oncogenic signaling by facilitating the export of mRNAs encoding key oncoproteins, such as MYC, BCL2, cyclin D1, and PIM1. In DLBCL, selective inhibitors of nuclear export (SINEs) have demonstrated potent preclinical and clinical efficacy by inducing the nuclear retention of tumor suppressor proteins, downregulating MYC expression, and triggering apoptotic pathways in malignant cells. Despite their promising therapeutic potential, the clinical application of XPO1 inhibitors has been limited by their dose-dependent toxicity. Given these insights, we aimed to explore the combination of A485 with XPO1 inhibitors to determine whether their complementary mechanisms could enhance therapeutic efficacy while mitigating toxicity in DLBCL treatment. To assess the dual effects of A485 combined with the XPO1 inhibitor KPT8602, the lymphoma cell line OCI-LY7 was simultaneously exposed to A485 and KPT8602 for 72 h at different concentrations. As shown in Fig. 5A, A485 at concentration of 400nM combined with KPT8602 at 10nM significantly inhibited DLBCL cell proliferation.

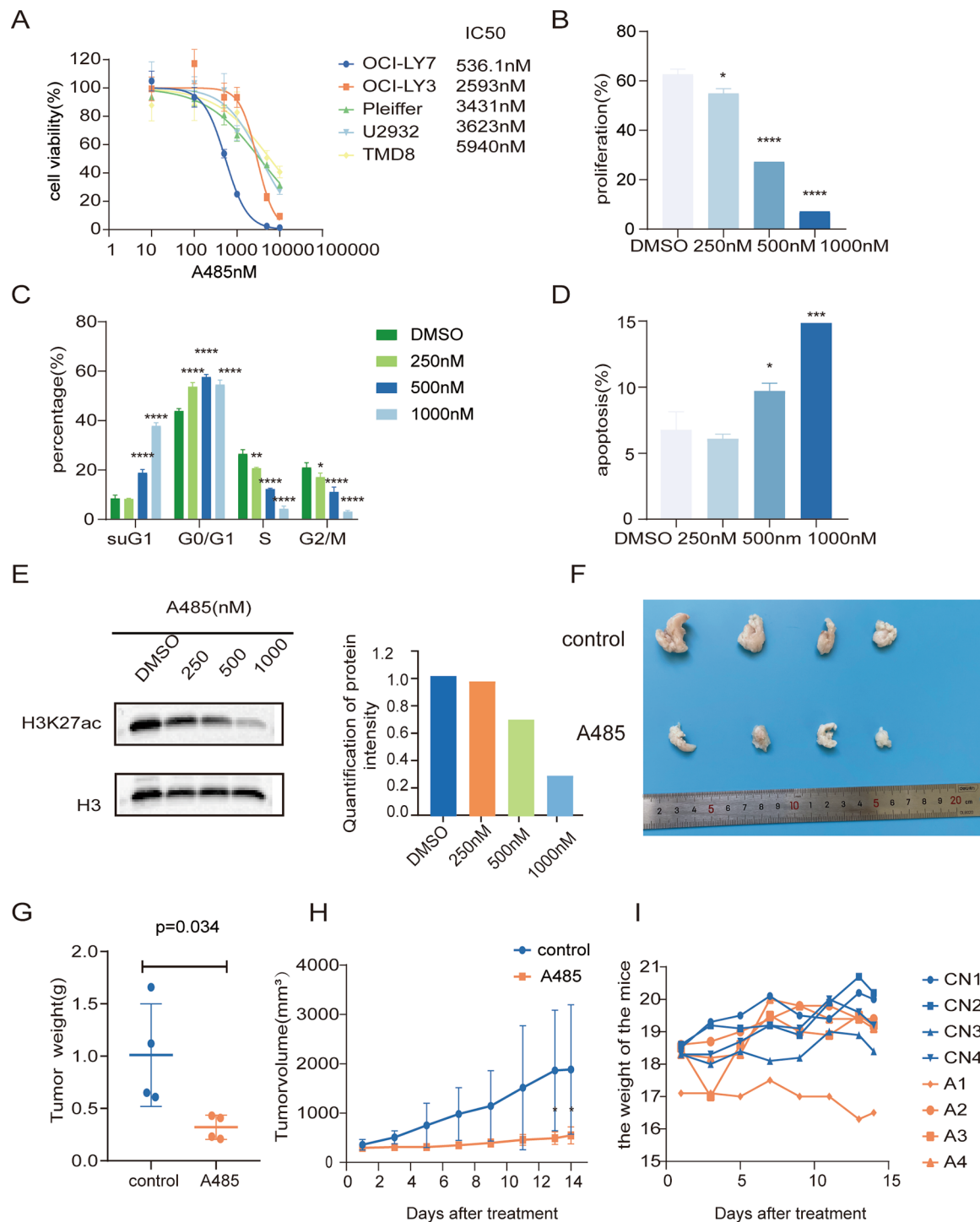


Fig. 2 EP300 Inhibitor A485 Induces Pan-Subtype Growth Arrest for DLBCL in vitro and in vivo. **A** Treatment with EP300 inhibitor A485 in human DLBCL cell lines leads to a significant reduction in cell viability. The viable cell numbers after A485 treatment are normalized as a percentage of the DMSO-treated control, with error bars representing the standard deviation (SD) from at least three independent experiments. **B-D** EP300 inhibitor A485 **B**) inhibits DLBCL cell proliferation by **C**) inducing cell-cycle arrest and **D**) apoptosis. **E** Quantification of histone modifications in DLBCL cells treated with EP300 inhibitor A485. **F-I** EP300 inhibitor treatment demonstrates promising therapeutic effects in vivo. **F**) Tumor volume and **G**) tumor weight in mice bearing DHL treated with A485. **H**) Representative images of tumors from the therapeutic study. **I**). Body weight of NSG OCI-LY7 cell recipients during a 14-day treatment with vehicle or A485

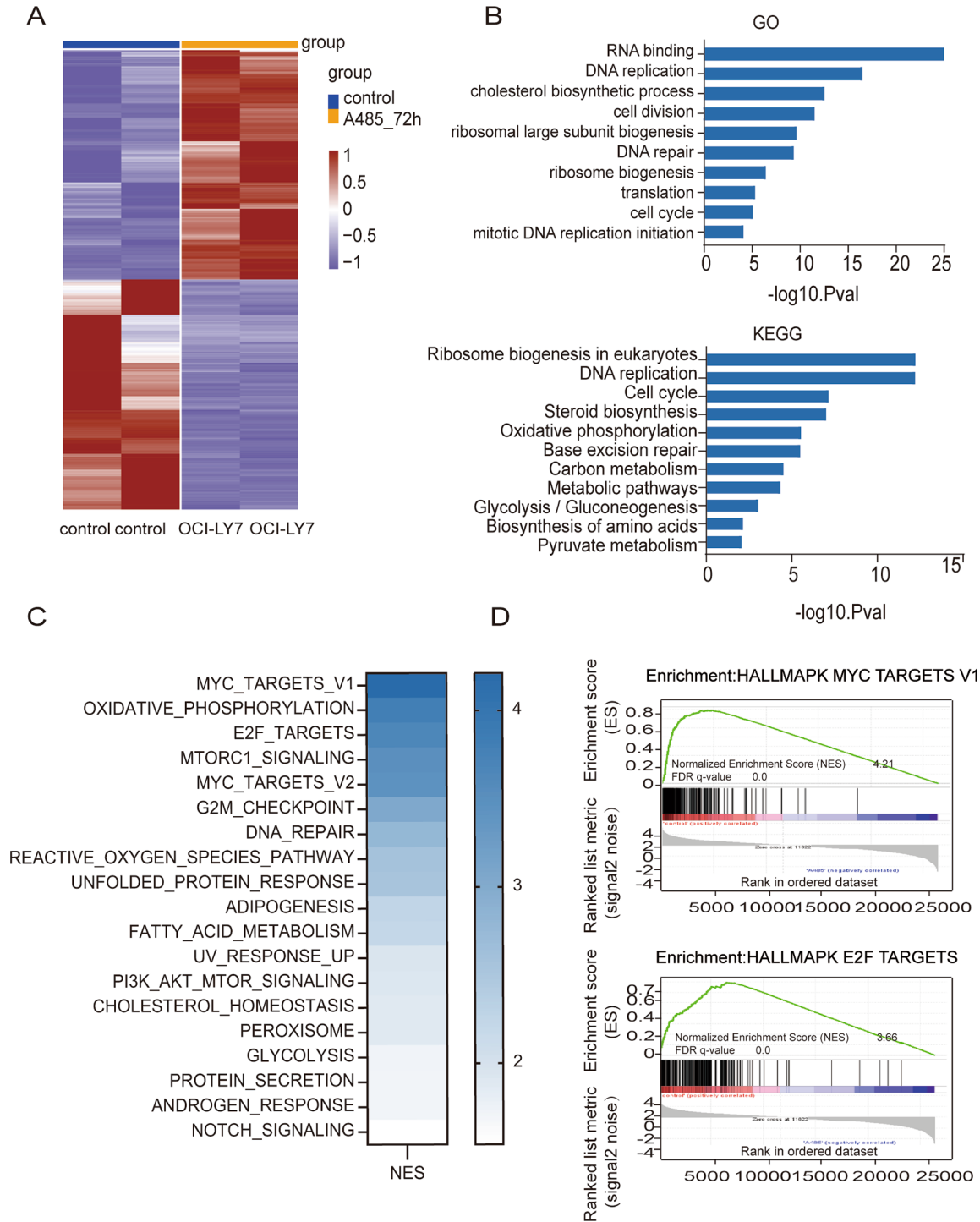


Fig. 3 Targeting EP300 Attenuates Lymphoma Cell Proliferation through Inhibition of C-MYC and E2F1 Signaling Pathways. **A** Heat map illustrating genome-wide transcriptional changes in control vs. A485 DLBCL cells, with three replicates. $FC \geq 0$, $FDR \leq 0.05$. **B** Comprehensive GO enrichment and KEGG enrichment analyses of downregulated genes in DLBCL cells after treatment with A485. **C** Gene set enrichment analysis with the hallmarks pathway from the Molecular Signatures Database ($FDR < 0.25$) in the DLBCL cell line. Normalized RNA-sequencing counts to identify overrepresented pathways, revealing de-enrichment post A485 treatment. **D** GSEA focusing on MYC targets and E2F1 targets in DLBCL cells treated with A485 and DMSO

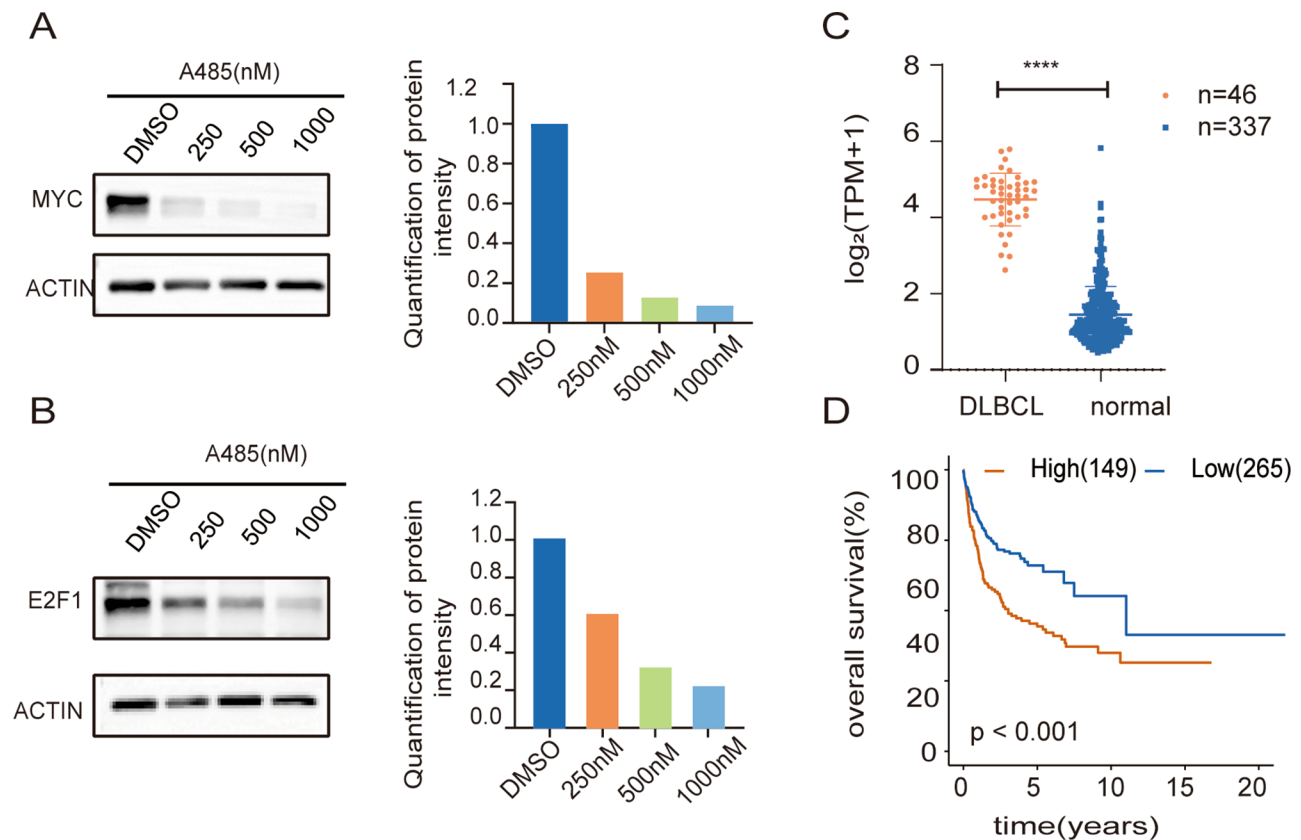


Fig. 4 Impact of EP300 Inhibitor A485 on E2F1. **A** Validated expression levels of MYC in DLBCL cell lines after A485 treatment using western blot analysis. **B** Western blot analysis validating E2F1 expression in DLBCL cell lines after A485 treatment. **C** Relative expression of E2F1 in normal and DLBCL tissues. **D** Kaplan-Meier curve comparing the overall survival of patients with DLBCL based on E2F1 expression

Next, we investigated whether the synergistic effect of the A485 and KPT8602 combination was due to the induction of apoptosis. As shown in Fig. 5B, A485 at concentration of 400nM combined with KPT8602 at 10nM, also significantly increased the rate of apoptosis in DLBCL cells compared to that in control cells. Encouraged by these results, we initiated an in vivo study to test the combination therapy. Lower doses of KPT8602 and A485 were selected as part of the therapeutic regimen. Tumor-bearing mice were randomized to receive vehicle, A485, KPT8602, or their combination. As predicted, significant decreases in tumor progression (Fig. 5C) and tumor weight (Fig. 5D) were observed in the combination group, while treatment with a single agent showed moderate effects. Combination treatment led to the highest synergy (Fig. 5E). Neither group experienced significant adverse effects, including treatment-related mortality or weight loss, suggesting that A485 combined with KPT8602 exerts a selective anti-lymphoma effect on human DLBCL cells in vivo.

Discussion

As a chromatin remodeling-related gene, EP300 is frequently overexpressed and is correlated with poor prognosis in patients with DLBCL. Repression of EP300 exerted its anti-lymphoma effect by restricting cell proliferation, facilitating cell cycle arrest, and inducing apoptosis through suppression of MYC and E2F1 pathway expression. Furthermore, treatment with EP300 and XPO1 inhibitors synergistically exhibited strong activity against DLBCL in vitro and in xenograft mouse models. These findings shed light on a novel epigenetic mechanism that contributes to the understanding of DLBCL progression and provide a theoretical basis for targeting EP300 in DLBCL therapy.

EP300 and CREBBP encode ubiquitously expressed mammalian enzymes that act as global transcriptional co-activators by interacting with more than 400 TFs and catalyzing the modification of lysine residues on both histone and non-histone proteins in a cell-context-dependent manner [24]. The HAT activity of EP300 is often aberrantly controlled in cancers, including hematological malignancies. Wei W et al. found that EP300, but not CREBBP, directly regulates oncogenic transcriptional programs and the expression of immunoregulatory

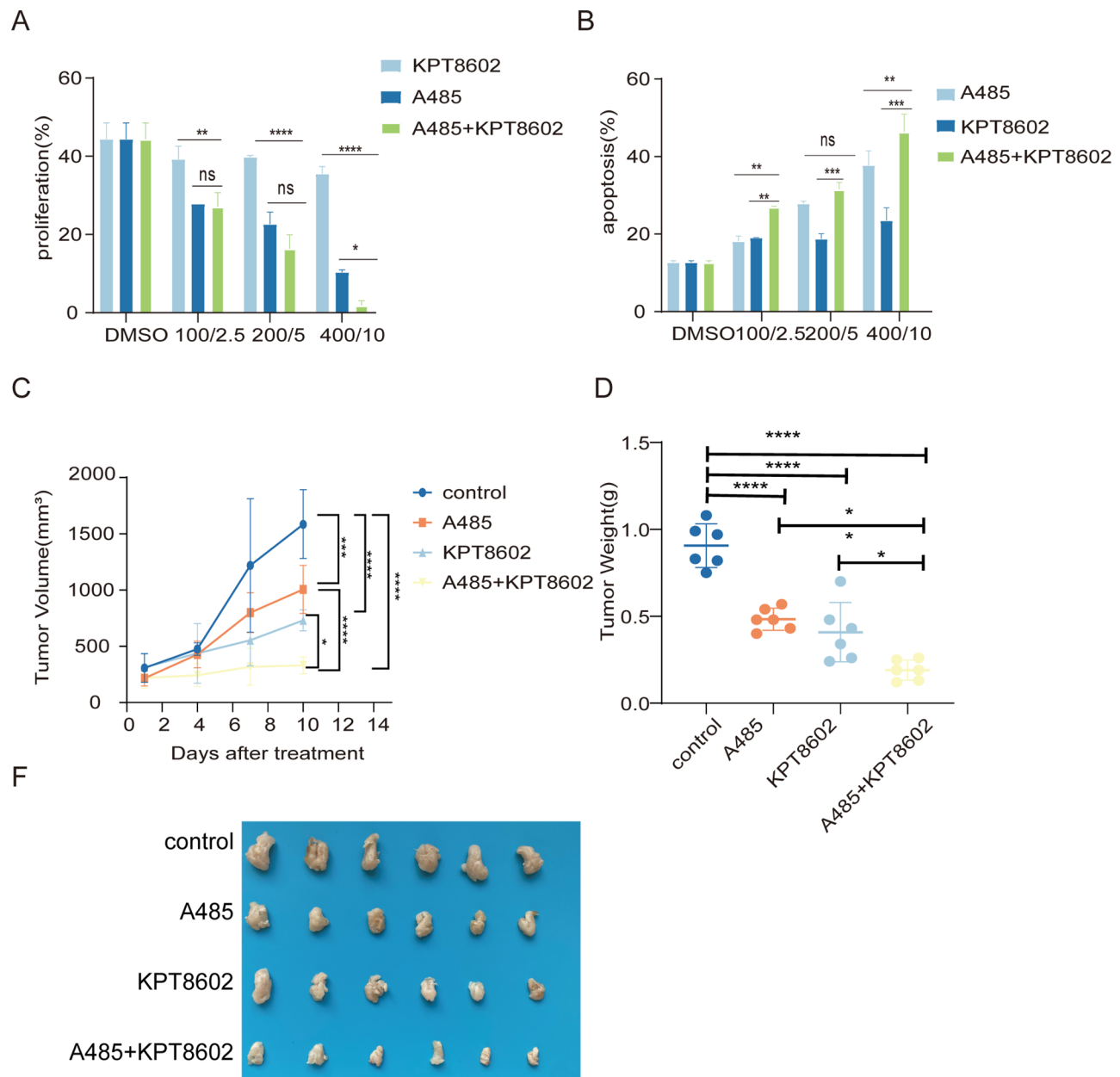


Fig. 5 Synergistic Therapeutic Strategy Simultaneously Targeting EP300 and XPO1 in DLBCL. **A** Inhibitory effect of combining the EP300 inhibitor with KPT8602 on the proliferation of lymphoma cells. **B** Pro-apoptotic impact of combining the EP300 inhibitor with KPT8602 on lymphoma cells. **C-E** The synergistic effect of combining the EP300 inhibitor with KPT8602 in vivo. **C-D** Tumor volume and tumor weight data for mice bearing OCI-LY7 cells treated with the control, A485, KPT8602, and combination groups. **E** Representative images of tumors from a therapeutic study

cytokines, immunosuppressive molecules, and surface receptors that shape the tumor microenvironment in anaplastic large cell lymphoma (ALCL) and classical Hodgkin lymphoma (HL) [25]. Durbin AD et al. demonstrated that EP300 controls oncogenic CRC-driven transcription in high-risk pediatric neuroblastoma (NB) by binding TFAP2 β [26]. Genomic analyses of DLBCL have revealed highly recurrent somatic mutations and deletions in CREBBP (25%), with much lower frequencies of EP300 [27]. Here, we found that EP300, but not CREBBP,

was overexpressed in patients with DLBCL, and that high expression of EP300 correlated with poor outcomes. We examined the relative dependency of EP300 and CREBBP in tumor cell lines using the DepMap exome-wide CRISPR-Cas9 deletion dataset. This demonstrated that most lymphoma cell lines require EP300 for cell growth, interestingly including DHL cell lines, whereas this phenomenon was not observed for CREBBP. These data provided a theoretical basis for the targeting of EP300 in DLBCL treatment.

A recent study reported that A485 [28], a selective EP300 inhibitor, attenuates proliferation in lineage-specific tumor types [29–31]. However, the effect of EP300 inhibitors on DLBCL remains unclear. In this study, we assessed the effect of A485, a potent inhibitor of DLBCL. We found that A485 decreased the levels of H3K27Ac and exhibited a therapeutic effect in DLBCL cells and a mouse model, suggesting that targeting EP300 might be a promising clinical strategy for DLBCL. Our gene expression analyses, and functional studies revealed that EP300 inhibition targeted the MYC and E2F1 pathways in DLBCL cells. MYC is a key oncogenic transcription factor regulated by super-enhancer regions containing EP300/CREBBP (identified by high densities of H3K27Ac). MYC plays a crucial role in hematological cancers, such as aggressive B-cell lymphoma [32], as well as in several solid tumors [33, 34]. MYC overexpression correlates with adverse outcomes in DLBCL [35]. Previous studies have shown that A485 robustly decreases MYC expression in many cancers, such as *myc*-amplified NB, prostate cancer, ALCL, and classical HL [18, 25, 26]. We speculated that A485 decreases MYC expression by regulating its H3K27 acetylation level in super-enhancer regions [36]. E2F1, a well-known transcription factor, promotes cell proliferation, inhibits apoptosis and differentiation, and facilitates DNA repair by upregulating HR-associated genes [37–39]. GSEA showed that A485 influenced the E2F1 target gene set. Moreover, we found that E2F1 was overexpressed in DLBCL tissues and that patients with DLBCL overexpressing E2F1 had worse OS. These data indicated that MYC and E2F1 are direct transcriptional targets of A485, required for proliferation and survival in DLBCL.

Interestingly, our study demonstrated that A485 modulates the expression of a set of metabolism-related genes, including those involved in cholesterol biosynthesis, steroid biosynthesis, carbon metabolism, glycolysis, and TCA. As previously shown, EP300/CREBBP promotes the transcription of metabolic enzyme genes by regulating H3K27Ac and H3K18Ac [10]. EP300 inhibitors attenuate HCC progression by decreasing the expression of genes involved in amino acid metabolism and nucleotide synthesis through epigenetic regulation [10]. Ma et al. have demonstrated that EP300 contributes to glucose metabolic reprogramming and malignant progression in lung cancer by catalyzing succinylation [40]. This finding indicated crosstalk between metabolism and epigenetic modifications, leading to a new understanding of the interrelationship between metabolism and epigenetics. However, the functional cooperation between EP300 and metabolism in DLBCL remains unknown. Further studies are required to verify the correlation between EP300 and metabolism in DLBCL.

Our study demonstrated for the first time that the combination of A485 and the XPO1 inhibitor KPT8602 exerted synergistic anti-lymphoma effects against DLBCL cells both *in vitro* and *in vivo*. This synergy was evident through enhanced inhibition of cell proliferation, increased apoptosis, and significant suppression of tumor progression in a DLBCL mouse model. Although we monitored body weight and general condition as indicators of toxicity, we recognize that further assessments, such as histopathological analyses would provide a more complete safety profile. XPO1 plays a critical role in cellular homeostasis and mediates the nuclear export of various cargoes, including proteins and RNAs [41]. Notably, patients with DLBCL and high XPO1 expression have significantly poorer OS and progression-free survival than those with low or undetectable XPO1 expression, highlighting the therapeutic potential of SINEs [42–43]. Despite these encouraging results, the precise molecular mechanisms underlying the synergistic effects remain unclear. One possible explanation for this is the complementary regulation of MYC, a key oncogene implicated in DLBCL pathogenesis. A485 suppresses MYC expression by altering MYC-dependent transcriptional regulation, leading to decreased MYC protein levels. XPO1 inhibitors have been shown to reduce MYC protein levels in various cancers, including hematological malignancies [44–48]. Notably, although the nuclear export of c-MYC is not mediated by CRM1, a recent study suggested that XPO1 exports eIF4E, a translation initiation factor that enhances c-MYC translation. Inhibition of XPO1 prevents eIF4E from promoting c-MYC translation [47]. Liu et al. also demonstrated that XPO1 inhibition significantly downregulates MYC protein expression, despite an increase in MYC mRNA levels. This suggests that MYC downregulation is not due to changes in mRNA levels or transport. And their further experiments ruled out protein degradation as a contributing factor, because a proteasome inhibitor did not prevent MYC downregulation [47]. Thus, XPO1 inhibition is likely to reduce MYC protein levels by inhibiting its translation. Based on the literature and our experiments, we propose that the synergy between A485 and KPT8602 arises from their complementary effects on MYC regulation—A485 affects MYC transcription, while XPO1 inhibition interferes with MYC translation, together leading to a synergistic reduction in MYC expression.

In addition to MYC regulation, the combination of A485 and KPT8602 may have a broader impact on critical signaling pathways in DLBCL. As an XPO1 inhibitor, KPT8602 may also affect the nuclear export of other key transcription factors, such as NF- κ B, p53, and FOXO3, which play critical roles in the pathogenesis of DLBCL [41]. The combination of A485 and KPT8602 may exert enhanced anti-tumor effects by simultaneously targeting

multiple key signaling pathways, thereby inhibiting tumor cell growth and reducing resistance. Given the promising therapeutic potential observed in our study, future studies are necessary to delineate these mechanisms and explore additional biomarkers predictive of response to combination therapy.

Conclusions

The current study demonstrated that EP300 contributed to DLBCL progression and poor prognosis. We found that EP300 inhibitors attenuated DLBCL progression, probably by inhibiting the MYC and E2F1 pathways. We further demonstrated that an EP300 inhibitor, alone or in combination with an XPO1 inhibitor, potently inhibited DLBCL cells in vitro and in vivo. These findings revealed a novel mechanism of epigenetic regulation by EP300 in DLBCL progression and highlighted the potential of EP300 as a therapeutic target and predictor of DLBCL.

Supplementary Information

The online version contains supplementary material available at <https://doi.org/10.1186/s12885-025-14257-y>.

Supplementary Material 1
Supplementary Material 2
Supplementary Material 3
Supplementary Material 4
Supplementary Material 5
Supplementary Material 6
Supplementary Material 7
Supplementary Material 8
Supplementary Material 9

Acknowledgements
N/A.

Author contributions

Conception and design were performed by ZGZ. The vitro experiments were performed by YNJ, DHX, and WQW. In addition, YNJ, WQW, CL, XH, and KPL conducted the experiments in vivo. WQW, YYL, JG, and HMS analyzed the results and wrote the manuscript. ZGZ and YNJ reviewed and edited the manuscript. JYN, and ZGZ revised the manuscript. Final approval of manuscript was performed by all authors who read and approved the final manuscript.

Funding

This work was supported by the key program of the Natural Science Foundation of Tianjin Province, China (23JCZDJC00340).

Data availability

The gene expression and clinical information of patients in the GSE10846 cohort were downloaded from <https://portal.gdc.cancer.gov>. The FPKM files of RNA-seq transcriptome data from 337 DLBCL tissues and 47 normal control tissues were obtained from the TCGA database to support the findings of this study. These data were analyzed using the GEPIA platform (<http://gepia.cancer-pku.cn/>). The data generated in this study are provided in the supplementary files. The remaining materials are available from the corresponding author upon reasonable request.

Declarations

Ethics approval and consent to participate

This study was reviewed and approved by the Research Ethics Committee of Tianjin Medical University Cancer Institute and Hospital. All animal experiments were approved by the Institutional Animal Care and Use Committee of the Tianjin Medical University Cancer Institute and Hospital.

Consent for publication

Not applicable.

Competing interests

The authors declare no competing interests.

Author details

¹Department of Medical Oncology, School of Medicine, Tianjin First Central Hospital, Nankai University, Tianjin 300192, China

²Key Laboratory of Cancer Prevention and Therapy, Tianjin Medical University Cancer Institute and Hospital, National Clinical Research Center for Cancer, Tianjin's Clinical Research Center for Cancer, Tianjin, China

³Department of Senior ward, Key Laboratory of Cancer Prevention and Therapy, Tianjin Medical University Cancer Institute and Hospital, National Clinical Research Center for Cancer, Tianjin's Clinical Research Center for Cancer, Tianjin 300060, China

Received: 21 January 2025 / Accepted: 2 May 2025

Published online: 28 May 2025

References

1. Bartlett NL, Wilson WH, Jung SH, Hsi ED, Maurer MJ, Pederson LD, Polley MC, Pitcher BN, Cheson BD, Kahl BS, et al. Dose-Adjusted EPOCH-R compared with R-CHOP as frontline therapy for diffuse large B-Cell lymphoma: clinical outcomes of the phase III intergroup trial Alliance/CALGB 50303. *J Clin Oncol*. 2019;37(21):1790–9.
2. Pfreundschuh M, Kuhnt E, Trümper L, Osterborg A, Trnety M, Shepherd L, et al. CHOP-like chemotherapy with or without rituximab in young patients with good-prognosis diffuse large-B-cell lymphoma: 6-year results of an open-label randomised study of the MabThera international trial (MINT) group. *Lancet Oncol*. 2011;12(11):1013–22.
3. Pfreundschuh M, Kuhnt E, Trümper L, Osterborg A, Trnety M, Shepherd L, Gill DS, Walewski J, Pettengell R, Jaeger U, et al. Higher response to Lenalidomide in relapsed/refractory diffuse large B-cell lymphoma in nongerminal center B-cell-like than in germinal center B-cell-like phenotype. *Cancer*. 2011;117(22):5058–66.
4. Zinzani PL, Thieblemont C, Melnichenko V, Bouabdallah K, Walewski J, Majlis A, Fogliatto L, Garcia-Sancho AM, Christian B, Gulbas Z, et al. Pembrolizumab in relapsed or refractory primary mediastinal large B-cell lymphoma: final analysis of KEYNOTE-170. *Blood*. 2023;142(2):141–5.
5. Frigault MJ, Armand P, Redd RA, Jeter E, Merryman RW, Coleman KC, Herrera AF, Dahi P, Nieto Y, LaCasce AS, et al. PD-1 Blockade for diffuse large B-cell lymphoma after autologous stem cell transplantation. *Blood Adv*. 2020;4(1):122–6.
6. Chen X, Lu T, Ding M, Cai Y, Yu Z, Zhou X, Wang X. Targeting YTHDF2 inhibits tumorigenesis of diffuse large B-cell lymphoma through ACER2-mediated ceramide catabolism. *J Adv Res*. 2023.
7. Clozel T, Yang S, Elstrom RL, Tam W, Martin P, Kormaksson M, Banerjee S, Vasanthakumar A, Culjkovic B, Scott DW, et al. Mechanism-based epigenetic chemosensitization therapy of diffuse large B-cell lymphoma. *Cancer Discov*. 2013;3(9):1002–19.
8. Geffen Y, Anand S, Akiyama Y, Yaron TM, Song Y, Johnson JL, Govindan A, Babur Ö, Li Y, et al. Pan-cancer analysis of post-translational modifications reveals shared patterns of protein regulation. *Cell*. 2023;186(18):3945–e39673926.
9. Li QL, Wang DY, Ju LG, Yao J, Gao C, Lei PJ, Li LY, Zhao XL, Wu M. The hyperactivation of transcriptional enhancers in breast cancer. *Clin Epigenetics*. 2019;11(1):48.
10. Cai LY, Chen SJ, Xiao SH, Sun QJ, Ding CH, Zheng BN, Zhu XY, Liu SQ, Yang F, Yang YX, et al. Targeting p300/CBP attenuates hepatocellular carcinoma progression through epigenetic regulation of metabolism. *Cancer Res*. 2021;81(4):860–72.

11. Totani H, Shinjo K, Suzuki M, Katsushima K, Mase S, Masaki A, Ito A, Ri M, Kusu-moto S, Komatsu H, et al. Autocrine HGF/c-Met signaling pathway confers aggressiveness in lymph node adult T-cell leukemia/lymphoma. *Oncogene*. 2020;39(35):5782–94.
12. Sungalee S, Liu Y, Lambuta RA, Katanayeva N, Donaldson Collier M, Tavernari D, Roulland S, Ciriello G. Oricchio e.histone acetylation dynamics modulates chromatin conformation and allele-specific interactions at oncogenic loci. *Nat Genet*. 2021;53(5):650–62.
13. Cui H, Hong Q, Wei R, Li H, Wan C, Chen X, Zhao S, Bu H, Zhang B, Yang D, et al. Design and synthesis of HDAC inhibitors to enhance the therapeutic effect of diffuse large B-cell lymphoma by improving metabolic stability and Pharmacokinetic characteristics. *Eur J Med Chem*. 2022;229:114049.
14. Mensah AA, Spriano F, Sartori G, Priebe V, Cascione L, Gaudio E, Tarantelli C, Civanelli E, Aresu L, Rinaldi A, et al. Study of the Antilymphoma activity of pracinostat reveals different sensitivities of DLBCL cells to HDAC inhibitors. *Blood Adv*. 2021;5(10):2467–80.
15. Wu C, Song Q, Gao S, Wu S. Targeting HDACs for diffuse large B-cell lymphoma therapy. *Sci Rep*. 2024;14(1):289.
16. Mondello P, Tadros S, Teater M, Fontan L, Chang AY, Jain N, Yang H, Singh S, Ying HY, Chu CS, et al. Selective Inhibition of HDAC3 targets synthetic vulnerabilities and activates immune surveillance in lymphoma. *Cancer Discov*. 2020;10(3):440–59.
17. Gou P, Zhang W. Protein lysine acetyltransferase CBP/p300: A promising target for small molecules in cancer treatment. *Biomed Pharmacother*. 2024;171:116130.
18. Welti J, Sharp A, Brooks N, Yuan W, McNair C, Chand SN, Pal A, Figueiredo I, Riisnaes R, Gurel B, et al. Targeting the p300/CBP Axis in lethal prostate Cancer. *Cancer Discov*. 2021;11(5):1118–37.
19. Pan F, Iwasaki M, Wu W, Jiang Y, Yang X, Zhu L, Zhao Z, Cleary ML, an, Iwasaki F, Wu M, Jiang W, Yang Y, Zhu X et al. Enhancer remodeling drives MLL oncogene-dependent transcriptional dysregulation in leukemia stem cells. *Blood Adv*. 2023; 7(11):2504–2519.
20. Szablewski V, Bret C, Kassambara A, Devin J, Cartron G, Costes-Martineau V, Moreaux J. An epigenetic regulator-related score (EpiScore) predicts survival in patients with diffuse large B cell lymphoma and identifies patients who May benefit from epigenetic therapy. *Oncotarget*. 2018;9(27):19079–99.
21. Reddy A, Zhang J, Davis NS, Moffitt AB, Love CL, Waldrop A, Leppa S, Pasanen A, Meriranta L, Karjalainen-Lindsberg ML, et al. Genetic and functional drivers of diffuse large B cell lymphoma. *Cell*. 2017;171(2):481–e494415.
22. Li Y, Xue M, Deng X, Dong L, Nguyen LXT, Ren L, Han L, Li C, Xue J, Zhao Z, et al. TET2-mediated mRNA demethylation regulates leukemia stem cell homing and self-renewal. *Cell Stem Cell*. 2023;30(8):1072–e10901010.
23. Fong CY, Morison J, Dawson MA. Epigenetics in the hematologic malignancies. *Haematologica*. 2014;99(12):1772–83.
24. Ogrzyzko VV, Schiltz RL, Russanova V, Howard BH, Nakatani Y. The transcriptional coactivators p300 and CBP are histone acetyltransferases. *Cell*. 1996;87(5):953–9.
25. Wei W, Song Z, Chiba M, Wu W, Jeong S, Zhang JP, Kadin ME, Nakagawa M, Yang Y. Analysis and therapeutic targeting of the EP300 and CREBBP acetyltransferases in anaplastic large cell lymphoma and hodgkin lymphoma. *Leukemia*. 2023;37(2):396–407.
26. Durbin AD, Wang T, Wimalasena VK, Zimmerman MW, Li D, Dharia NV, Mariani L, Shendy NAM, Nance S, Patel AG, et al. EP300 selectively controls the enhancer landscape of MYCN-Amplified neuroblastoma. *Cancer Discov*. 2022;12(3):730–51.
27. Meyer SN, Scuoppo C, Vlashevsk S, Bal E, Holmes AB, Holloman M, Garcia-Ibanez L, Nataraj S, Duval R, Vantrimpont T, et al. Unique and shared epigenetic programs of the CREBBP and EP300 acetyltransferases in germinal center B cells reveal targetable dependencies in lymphoma. *Immunity*. 2019;51(3):535–e547539.
28. Lasko LM, Jakob CG, Edalji RP, Qiu W, Montgomery D, Digiammarino EL, Hansen TM, Risi RM, Frey R, Manaves V, et al. Discovery of a selective catalytic p300/CBP inhibitor that targets lineage-specific tumours. *Nature*. 2017;550(7674):128–32.
29. Zhou F, Liu Q, Zhang L, Zhu Q, Wang S, Zhu K, Deng R, Liu Y, Yuan G, Wang X, et al. Selective Inhibition of CBP/p300 HAT by A-485 results in suppression of lipogenesis and hepatic gluconeogenesis. *Cell Death Dis*. 2020;11(9):745.
30. Zhang X, Zegar T, Lucas A, Morrison-Smith C, Knox T, French CA, Knapp S, Müller S, Sivek JT. Therapeutic targeting of p300/CBP HAT domain for the treatment of NUT midline carcinoma. *Oncogene*. 2020;39(24):4770–9.
31. Ji C, Xu W, Ding H, Chen Z, Shi C, Han J, Yu L, Qiao N, Zhang Y, Cao X, et al. The p300 inhibitor A-485 exerts antitumor activity in growth hormone pituitary adenoma. *J Clin Endocrinol Metab*. 2022;107(6):e2291–300.
32. Ott G, Rosenwald A, Campo E. Understanding MYC-driven aggressive B-cell lymphomas: pathogenesis and classification. *Blood*. 2013;122(24):3884–91.
33. Dimova I, Raitcheva S, Dimitrov R, Doganov N, Toncheva D. Correlations between c-myc gene copy-number and clinicopathological parameters of ovarian tumours. *Eur J Cancer*. 2006;42(5):674–9.
34. Papadimitropoulou A, Makri M, Zoidis G. MYC the oncogene from Hell: novel opportunities for cancer therapy. *Eur J Med Chem*. 2024;267:116194.
35. Gupta M, Maurer MJ, Welik LE, Law ME, Han JJ, Ozsan N, Micallef IN, Dogan A, Witzig TE. Expression of Myc, but not pSTAT3, is an adverse prognostic factor for diffuse large B-cell lymphoma treated with epratuzumab/R-CHOP. *Blood*. 2012;120(22):4400–6.
36. Hnisz D, Abraham BJ, Lee TI, Lau A, Saint-André V, Sigova AA, Hoke HA, Young RA. Super-enhancers in the control of cell identity and disease. *Cell*. 2013;155(4):934–47.
37. Wang Y, Deng O, Feng Z, Du Z, Xiong X, Lai J, Yang X, Xu M, Wang H, Taylor D, et al. RNF126 promotes homologous recombination via regulation of E2F1-mediated BRCA1 expression. *Oncogene*. 2016;35(11):1363–72.
38. Guo D, Zhao Y, Wang N, You N, Zhu W, Zhang P, Ren Q, Yin J, Cheng T, Ma X. GADD45g acts as a novel tumor suppressor, and its activation suggests new combination regimens for the treatment of AML. *Blood*. 2021;138(6):464–79.
39. Degregori J. A new role for E2F1 in DNA repair: all for the greater good. *Cell Cycle*. 2011;10(11):1716.
40. Ma Q, Zeng Q, Wang K, Qian M, Li J, Wang H, Zhang H, Jiang J, Chen Z, Huang W. Acetyltransferase P300 regulates glucose metabolic reprogramming through catalyzing succinylation in lung Cancer. *Int J Mol Sci*. 2024; 25(2).
41. Azmi AS, Uddin MH, Mohammad RM. The nuclear export protein XPO1 - from biology to targeted therapy. *Nat Rev Clin Oncol*. 2021;18(3):152–69.
42. Deng M, Zhang M, Xu-Monette ZY, Pham LV, Tzankov A, Visco C, Fang X, Bhagat G, Zhu F, Dybkaer K, et al. XPO1 expression worsens the prognosis of unfavorable DLBCL that can be effectively targeted by Selinexor in the absence of mutant p53. *J Hematol Oncol*. 2020;13(1):148.
43. Ben-Barouch S, Kuruvilla J. Selinexor (KTP-330) - a selective inhibitor of nuclear export (SINE): anti-tumor activity in diffuse large B-cell lymphoma (DLBCL). *Expert Opin Investig Drugs*. 2020;29(1):15–21.
44. Tai YT, Landesman Y, Acharya C, Calle Y, Zhong MY, Cea M, Tannenbaum D, Cagnetta A, Reagan M, Munshi AA, et al. CRM1 Inhibition induces tumor cell cytotoxicity and impairs osteoclastogenesis in multiple myeloma: molecular mechanisms and therapeutic implications. *Leukemia*. 2014;28(1):155–65.
45. Zheng Y, Gery S, Sun H, Shacham S, Kauffman M, Koeffler HP. KPT-330 inhibitor of XPO1-mediated nuclear export has anti-proliferative activity in hepatocellular carcinoma. *Cancer Chemother Pharmacol*. 2014;74(3):487–95.
46. Ou L, Wang X, Cheng S, Zhang M, Cui R, Hu C, Liu S, Tang Q, Peng Y, Chai R, et al. Verdinexor, a selective inhibitor of nuclear exportin 1, inhibits the proliferation and migration of esophageal Cancer via XPO1/c-Myc/FOSL1 Axis. *Int J Biol Sci*. 2022;18(1):276–91.
47. Long H, Hou Y, Li J, Song C, Ge Z. Azacitidine is synergistically lethal with XPO1 inhibitor Selinexor in acute myeloid leukemia by targeting XPO1/ eIF4E/c-MYC signaling. *Int J Mol Sci*. 2023;24(7):6816.
48. Liu Y, Azizian NG, Dou Y, Pham LV, Li Y. Simultaneous targeting of XPO1 and BCL2 as an effective treatment strategy for double-hit lymphoma. *J Hematol Oncol*. 2019;12(1):119.

Publisher's note

Springer Nature remains neutral with regard to jurisdictional claims in published maps and institutional affiliations.